The Analysis on Transmission Characteristics of 25Hz Phase-sensitive Track Circuit in Broken State

FENG CHANG
Key Laboratory of Opto-Technology and Intelligent Control Ministry of Education
Lanzhou Jiaotong University
WENZHEN KUANG
College of Automation & Electrical Engineering
Lanzhou Jiaotong University
RUICHENG ZHAO
School of Traffic and Transportation
Lanzhou Jiaotong University
NO.88 AnNing West Anenue, Lanzhou, GanSu
CHINA
123cf88@163.com

Abstract: - 25Hz phase-sensitive track circuit has become the first selection of coded track circuit in railway station. The transmission characteristics of 25Hz phase-sensitive track circuit in broken state for analysis under the premise of considering the choke transformer. Take into account the impact of the choke transformer and adjacent track sections fully, and join the equivalent input impedance between the midpoint of the starting and the end of the rail line and the earth. Then the four terminal network model of the track circuit in broken state is established. And application of the distributed parameter method to solve the four terminal network coefficient of track circuit in the condition of broken state. Then, the transmission characteristics of the track circuit in broken state is carried out simulation analysis by using MATLAB simulation software. The simulation results show that broken rail state of track circuit power supply terminal voltage and current with position of broken rail, rail surface conductance and ballast resistance are related closely. Finally, according to the results of simulation analysis, the method of improving the sensitivity of the track circuit in broken state is proposed. The specific measures include: reducing the length of track circuit properly, increasing ballast resistance, increasing the rail surface conductance coefficient.

Key-Words: - Phase-sensitive track circuit, Transmission characteristic, Distribution parameter, Broken rail state

1 Introduction

With the increase of the train running speed, the state of the track circuit has become a major barrier of the train running safety. When the track circuit in the broken state, the electrical characteristics of the sending and receiving terminal should be changed greatly. It is necessary to have sufficient capacity to detect and protect its broken rail, which requires the receiver to receive signals should be less than its receiving threshold under the condition of the track circuit in broken state. And detection of the occurrence of the broken rail promptly and shut it down automatically. Prevent the train from entering, effectively prevent the accidents which caused by the broken rail.

Research on the detection of broken track has a long history both domestic and foreign, and many results have been obtained in the method of broken rail detection. In the late 1980s in our country has introduced the UM71 joint-less track circuit which was researched and developed by French CSEE company. And on the basis, the ZPW2000 series of joint-less track circuit is developed, which has the function of all the broken rail detection [1,2]. In 1997, Shooman proposed a method to detect the broken track by using a traction reflux [3]. There are defects in the traction reflux detection method, which can only be detected by the track of the train entering the detection range and the traction reflux flow over the two track. This method is not suitable for operating line in the railway station. Ultrasonic testing is often used broken rail detection, which is based on the principle of mechanical wave [4-6]. Based on ultrasonic detection method of broken rail track, the rail flaw detector needs more manpower. And the high speed rail inspection car cost is high, so it does not apply to the busy station. Optical fiber detection as a high-sensitivity detection method, and it can be used in short track detection [7,8].

In the paper [9]and [10], modeling and simulation of track circuit with ballast-less track. However, this kind of track circuit is different from the structure of the ballast-less track circuit. So the model is not suitable for the current ballast-less track circuit. The influence of the equivalent circuit parameters of the receiving end of the circuit is mainly analyzed in the paper [11]. The paper [12] models and analyzes the on the broken rail mode of a track circuit of center-fed double-side current-received type. However, the structure of this kind of track circuit is special, so its modeling and analysis is not suitable for other track circuits. The receiver signal of an audio track circuit under the condition of the broken state is analyzed and calculated by paper [13] and [14]. However, this method does not take into account the impact of track-bed conditions. In the paper [15], the model of mechanical insulation track circuit is modeled by using the small and distributed parameter model. Regard it as a uniform transmission line, which is used to analyze the non-uniform distribution parameters. The uniform transmission line theory is an effective method to analyze the distributed parameter circuits.

2. Four-terminal Network Model of Chock Transformer and Track Circuit

2.1.1 Four-terminal Network for Solving the Coefficients of Choke Transformer

Choke transformer equivalent circuit as shown in Fig. 1, the equivalent circuit consists of three parts: the ideal autotransformer, T-type equivalent circuit and ideal transformer turns ratio of ($2N_T$:N_2). Where Z_1 is the magnetic flux leakage impedance of the traction winding (the number of turns is $2N_T$). Z_2' is the magnetic flux leakage impedance of the signal winding is converted to traction windings, and Z_m is converted to the traction windings of the excitation impedance [16].

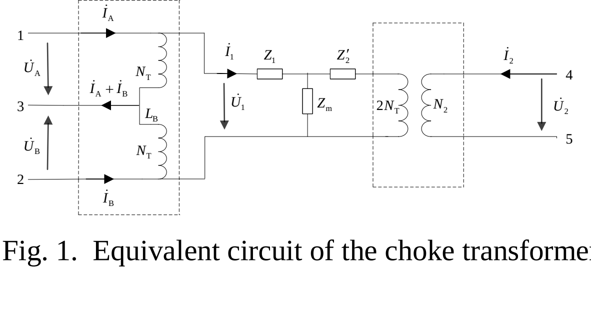

Fig. 1. Equivalent circuit of the choke transformer

We can know from Fig. 1 that four-terminal network of the choke transformer is a type of T network, as shown in Fig. 2 [17].

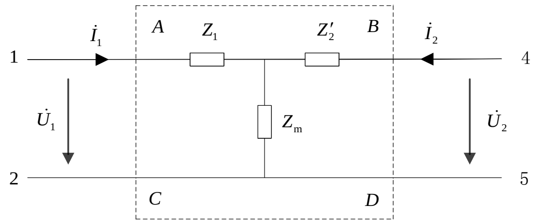

Fig. 2. T-type equivalent circuit of choke transformer

For a T-type network, because we know the value of the excitation and leakage impedance, so the four-terminal network choke transformer coefficient is,

$$\begin{cases} A = \left.\dfrac{\dot{U}_1}{\dot{U}_2}\right|_{\dot{I}_2=0} = \dfrac{Z_1 + Z_m}{Z_m} \\ B = \left.\dfrac{\dot{U}_1}{\dot{I}_2}\right|_{\dot{U}_2=0} = Z_1 + Z_2' + \dfrac{Z_1 \cdot Z_2'}{Z_m} \\ C = \left.\dfrac{\dot{I}_1}{\dot{U}_2}\right|_{\dot{I}_2=0} = \dfrac{1}{Z_m} \\ D = \left.\dfrac{\dot{I}_1}{\dot{I}_2}\right|_{\dot{U}_2=0} = \dfrac{Z_m + Z_2'}{Z_m} \end{cases} \quad (1)$$

2.1.2 Distributed Parameter Model of Track Circuit [18,19]

Track circuit is a circuit with uniform distribution parameters, which is characterized by two-way asymmetric leakage current. One-way current from the rail leak into the earth directly, the other way current through ballast and sleepers surface leakage by a single rail to the other.

We can regard the two rails and the earth as a circuit composed of three wires by using the distributed parameter method for the track circuit modeling. The earth can be considered as the conductor of the infinite area. These three wires are connected by a uniform distribution of leakage of g_1, g_2 and g_{12}. The equivalent circuit of a short circuit dx of the track circuit, as shown in Fig. 3.

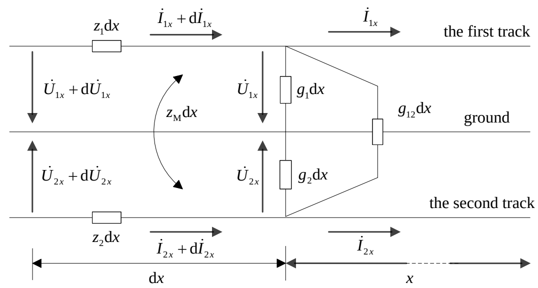

Fig. 3. Equivalent circuit of short dx for track line

In Fig. 3, z_1, z_2 for the single rail impedance ratio (Ω), g_1 and g_2 are the specific conductance of the rail to the ground (S). g_{12} is the conductance of a ballast surface and sleepers (S). z_M is a mutual impedance between two rails (Ω). x is the distance between the connecting load and the rail line terminal (m). I_{1x} and I_{2x} respectively represent the current in the two rails, which is the positive direction by the supply terminal to load (A). $\dot{U}_{1x}$ and $\dot{U}_{2x}$ respectively represent the voltage of two rails to the ground, the positive direction from rail to the ground (V).

According to Kirchhoff's law, a short dx of the rail line can be expressed as,

$$\begin{cases} \dot{U}_{1x} + \mathrm{d}\dot{U}_{1x} - \dot{U}_{1x} = z_1 \mathrm{d}x\dot{I}_{1x} + z_{\mathrm{M}}\mathrm{d}x\dot{I}_{2x} \\ \dot{U}_{2x} + \mathrm{d}\dot{U}_{2x} - \dot{U}_{2x} = z_2 \mathrm{d}x\dot{I}_{2x} + z_{\mathrm{M}}\mathrm{d}x\dot{I}_{1x} \\ \dot{I}_{1x} + \mathrm{d}\dot{I}_{1x} - \dot{I}_{1x} = g_1 \mathrm{d}x\dot{U}_{1x} + g_{12}\mathrm{d}x\dot{U}_{1x} - g_{12}\mathrm{d}x\dot{U}_{2x} \\ \dot{I}_{2x} + \mathrm{d}\dot{I}_{2x} - \dot{I}_{2x} = g_2 \mathrm{d}x\dot{U}_{2x} + g_{12}\mathrm{d}x\dot{U}_{2x} - g_{12}\mathrm{d}x\dot{U}_{1x} \end{cases} \tag{2}$$

The formula (2) is obtained as follows:

$$\dot{U}_{1x} = A_1 \cosh\gamma_1 x + A_2 \sinh\gamma_1 x + A_3 \cosh\gamma_2 x + A_4 \sinh\gamma_2 x \tag{3}$$

$$\begin{aligned} \dot{U}_{2x} &= M\left(A_1 \cosh\gamma_1 x + A_2 \sinh\gamma_1 x\right) \\ &\quad + N\left(A_3 \cosh\gamma_2 x + A_4 \sinh\gamma_2 x\right) \end{aligned} \tag{4}$$

$$\begin{aligned} \dot{I}_{1x} &= y_{11}\left(A_1 \sinh\gamma_1 x + A_2 \cosh\gamma_1 x\right) \\ &\quad + y_{12}\left(A_3 \sinh\gamma_2 x + A_4 \cosh\gamma_2 x\right) \end{aligned} \tag{5}$$

$$\begin{aligned} \dot{I}_{2x} &= y_{21}\left(A_1 \sinh\gamma_1 x + A_2 \cosh\gamma_1 x\right) \\ &\quad + y_{22}\left(A_3 \sinh\gamma_2 x + A_4 \cosh\gamma_2 x\right) \end{aligned} \tag{6}$$

where,

$$\gamma_1 = \sqrt{\frac{1}{2}a_1 - \sqrt{\frac{1}{4}a_1^2 - a_2}}\ ,\ \gamma_2 = \sqrt{\frac{1}{2}a_1 + \sqrt{\frac{1}{4}a_1^2 - a_2}}\ ;$$

A_1, A_2, A_3, A_4 is a constant of integration;

$$M = \frac{\gamma_1^2 - z_1\left(g_1 + g_{12}\right) + z_{\mathrm{M}}g_{12}}{z_{\mathrm{M}}\left(g_2 + g_{12}\right) - z_1 g_{12}}\ ,\ N = \frac{\gamma_2^2 - z_1\left(g_1 + g_{12}\right) + z_{\mathrm{M}}g_{12}}{z_{\mathrm{M}}\left(g_2 + g_{12}\right) - z_1 g_{12}}\ ;$$

$$a_1 = g_{12}\left(z_1 + z_2 - 2z_{\mathrm{M}}\right) + g_1 z_1 + g_2 z_2\ ;$$

$$a_2 = \left(z_1 z_2 - z_{\mathrm{M}}^2\right)\left(g_1 g_2 + g_1 g_{12} + g_2 g_{12}\right);$$

$$y_{11} = \gamma_1 \frac{z_2 - \mathrm{M}z_{\mathrm{M}}}{z_1 z_2 - z_{\mathrm{M}}^2}\ ,\ y_{12} = \gamma_2 \frac{z_2 - Nz_{\mathrm{M}}}{z_{12} - z_{\mathrm{M}}^2}\ ,$$

$$y_{21} = \gamma_1 \frac{Mz_1 - z_{\mathrm{M}}}{z_1 z_2 - z_{\mathrm{M}}^2}\ ,\ y_{21} = \gamma_2 \frac{Nz_1 - z_{\mathrm{M}}}{z_1 z_2 - z_{\mathrm{M}}^2}\ .$$

2.1.3 Solving the Four-terminal Network Coefficients of Track Circuit in Broken State

The equivalent circuit of the four-terminal network of the track circuit in broken state is shown in Fig. 4. Taking into account the influence of the adjacent track section, in the beginning and end of the rail line, the Z_{HBX} and Z_{KBX} are respectively connected with the neutral point of the ideal self-coupling transformer. Z_{HBX} and Z_{KBX} represent the input impedance of adjacent track section between the transformer and choke point of the earth. So the equivalent input impedance Z_{BXH} and Z_{HBX} of the elements and the ideal autotransformer connected to the beginning of the equivalent circuit. The equivalent output impedance of the Z_{BXK} and Z_{KBX} of the various components which are connected with the ideal self-coupling transformer are also present in the terminal.

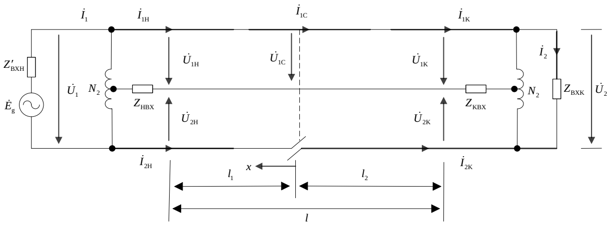

Fig. 4. Equivalent circuit of four-terminal network of the track circuit in broken state

The track circuit is considered as the boundary between the two four-terminal networks at the time of track circuit in broken state. The first half of the track circuit is represented by N_{11}, second half of the track circuit is represented by N_{22}. The connection of the four-terminal network of the track circuit in broken state is shown in Fig. 5.

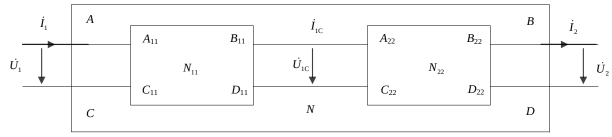

Fig. 5. The connection of the four-terminal network of the track circuit in broken state

The voltage of the broken rail to the ground is indicated by $\dot{U}_{1\mathrm{C}}$, internal current represented by $\dot{I}_{1\mathrm{C}}$. Therefore, the following equation was established,

$$\begin{cases} \dot{U}_{1\mathrm{C}} = A_{22}\dot{U}_2 + B_{22}\dot{I}_2 \\ \dot{I}_{1\mathrm{C}} = C_{22}\dot{U}_2 + D_{22}\dot{I}_2 \end{cases} \tag{7}$$

$$\begin{cases} \dot{U}_1 = A_{11}\dot{U}_{1\mathrm{C}} + B_{11}\dot{I}_{1C} \\ \dot{I}_1 = C_{11}\dot{U}_{1\mathrm{C}} + D_{11}\dot{I}_{1C} \end{cases} \tag{8}$$

The equations between the power supply and the receiving terminal are established as follows:

$$\begin{cases} \dot{U}_1 = A\dot{U}_2 + B\dot{I}_2 \\ \dot{I}_1 = C\dot{U}_2 + D\dot{I}_2 \end{cases} \tag{9}$$

Because the four-terminal network N is composed of N_{11} and N_{22}, there is the relationship can be expressed as:

$$\begin{bmatrix} A & B \\ C & D \end{bmatrix} = \begin{bmatrix} A_{11} & B_{11} \\ C_{11} & D_{11} \end{bmatrix} \cdot \begin{bmatrix} A_{22} & B_{22} \\ C_{22} & D_{22} \end{bmatrix} \tag{10}$$

Substituting $x = 0$ and $\dot{I}_{2x} = 0$ in (6), and can be obtained,

$$y_{21}A_2 + y_{22}A_4 = 0 \tag{11}$$

Substituting $x=0$ and $\dot{I}_{1x}=\dot{I}_{1C}$ in (5), and can be obtained,

$$y_{11}A_2 + y_{12}A_4 = \dot{I}_{1C} \tag{12}$$

Substituting $x=0$ and $\dot{U}_{1x}=\dot{U}_{1C}$ in (3), and can be obtained,

$$A_1 + A_3 = \dot{U}_{1C} \tag{13}$$

In the same method as described above Fig.4 and can be obtained,

$$\dot{U}_{1H} + \dot{U}_{2H} + 2Z_{HBX}\left(\dot{I}_{1H} + \dot{I}_{2H}\right) = 0 \tag{14}$$

Put $x=l_1$ into formula (3) to (6), $\dot{U}_{1H}$, $\dot{U}_{2H}$, $\dot{I}_{1H}$ and $\dot{I}_{2H}$ can be obtained, and then the equation can be obtained,

$$k_1A_1 + k_2A_2 + k_3A_3 + k_4A_4 = 0 \tag{15}$$

where,

$$\begin{cases} k_1 = (1+M)\cosh\gamma_1 l_1 + 2Z_{HBX}(y_{11}+y_{21})\sinh\gamma_1 l_1 \\ k_2 = (1+M)\sinh\gamma_1 l_1 + 2Z_{HBX}(y_{11}+y_{21})\cosh\gamma_1 l_1 \\ k_3 = (1+N)\cosh\gamma_2 l_1 + 2Z_{HBX}(y_{12}+y_{22})\sinh\gamma_2 l_1 \\ k_4 = (1+N)\sinh\gamma_2 l_1 + 2Z_{HBX}(y_{12}+y_{22})\cosh\gamma_2 l_1 \end{cases} \tag{16}$$

In the case of rail line symmetry,

$$M=1,\ N=-1,\ y_{11}=y_{21}=\frac{1}{Z_{B1}},\ y_{12}=-y_{22}=\frac{1}{Z_{B2}} \tag{17}$$

$$Z_{B1}=\frac{1}{2}EZ_B\sqrt{1+P},\ Z_{B2}=\frac{1}{2}Z_B,\ Z_{KBX}=Z_{HBX}=\frac{1}{2}Z_{B1} \tag{18}$$

Substituting (17) in (11), (12), (13) and (15),

$$\begin{cases} A_1 + A_3 = \dot{U}_{1C} \\ \frac{1}{Z_{B1}}A_2 + \frac{1}{Z_{B2}}A_4 = \dot{I}_{1C} \\ \frac{1}{Z_{B1}}A_2 - \frac{1}{Z_{B2}}A_4 = 0 \\ k_1A_1 + k_2A_2 + k_3A_3 + k_4A_4 = 0 \end{cases} \tag{19}$$

From (19), the equivalent can be expressed as,

$$\begin{bmatrix} 1 & 0 & 1 & 0 \\ 0 & \frac{1}{Z_{B1}} & 0 & \frac{1}{Z_{B2}} \\ 1 & \frac{1}{Z_{B1}} & 0 & -\frac{1}{Z_{B2}} \\ k_1 & k_2 & k_3 & k_4 \end{bmatrix}\begin{bmatrix} A_1 \\ A_2 \\ A_3 \\ A_4 \end{bmatrix} = \begin{bmatrix} \dot{U}_{1C} \\ \dot{I}_{1C} \\ 0 \\ 0 \end{bmatrix} \tag{20}$$

The upper formula is solved and obtained:

$$\begin{bmatrix} A_1 \\ A_2 \\ A_3 \\ A_4 \end{bmatrix} = \begin{bmatrix} A_{11} & A_{21} & A_{31} & A_{41} \\ A_{12} & A_{22} & A_{21} & A_{21} \\ 1 & \frac{Z_{B1}}{2} & A_{33} & A_{43} \\ 0 & \frac{Z_{B2}}{2} & A_{34} & A_{44} \end{bmatrix}\begin{bmatrix} \dot{U}_{1C} \\ \dot{I}_{1C} \\ 0 \\ 0 \end{bmatrix} \tag{21}$$

The formula (21) is further solved,

$$A_3 = \dot{U}_{1C} + \frac{Z_{B1}}{2}\dot{I}_{1C} \tag{22}$$

$$A_4 = \frac{Z_{B2}}{2}\dot{I}_{1C} \tag{23}$$

Substituting $x=l_1$ in (3), (4), (5) and (6), $\dot{U}_{1H}$, $\dot{U}_{2H}$, $\dot{I}_{1H}$ and $\dot{I}_{2H}$ can be obtained, and then the equation can be obtained, $\dot{U}_1$ and $\dot{I}_1$ can be expressed as,

$$\begin{aligned} \dot{U}_1 = &(1-M)(A_1\cosh\gamma_1 l_1 + A_2\sinh\gamma_1 l_1) \\ &+(1-N)(A_3\cosh\gamma_2 l_1 + A_4\sinh\gamma_2 l_1) \end{aligned} \tag{24}$$

$$\begin{aligned} \dot{I}_1 = &\frac{1}{2}[(y_{11}-y_{21})(A_1\sinh\gamma_1 l_1 + A_2\cosh\gamma_1 l_1) \\ &+(y_{12}-y_{22})(A_3\sinh\gamma_2 l_1 + A_4\cosh\gamma_2 l_1)] \end{aligned} \tag{25}$$

Substituting (17) and $\gamma_2=\gamma$ in (24) and (25), $\dot{U}_1$ and $\dot{I}_1$ can be simplified as,

$$\dot{U}_1 = 2(A_3\cosh\gamma l_1 + A_4\sinh\gamma l_1) \tag{26}$$

$$\dot{I}_1 = \frac{1}{Z_{B2}}(A_3\sinh\gamma l_1 + A_4\cosh\gamma l_1) \tag{27}$$

Substituting (22) and (23) in (26) and (27), $\dot{U}_1$ and $\dot{I}_1$ can be simplified as,

$$\dot{U}_1 = 2\cosh(\gamma l_1)\dot{U}_{1C} + (Z_{B1}\cosh\gamma l_1 + Z_{B2}\sinh\gamma l_1)\dot{I}_{1C} \tag{28}$$

$$\dot{I}_1 = \frac{1}{Z_{B2}}\sinh(\gamma l_1)\dot{U}_{1C} + \frac{1}{2}\left(\frac{Z_{B1}}{Z_{B2}}\sinh\gamma l_1 + \cosh\gamma l_1\right)\dot{I}_{1C} \tag{29}$$

Four-terminal network N_{11} coefficients are as follows,

$$\begin{cases} A_{11} = 2\cosh\gamma l_1 \\ B_{11} = Z_{B1}\cosh\gamma l_1 + Z_{B2}\sinh\gamma l_1 \\ C_{11} = \frac{1}{Z_{B2}}\sinh\gamma l_1 \\ D_{11} = \frac{1}{2}\left(\frac{Z_{B1}}{Z_{B2}}\sinh\gamma l_1 + \cosh\gamma l_1\right) \end{cases} \tag{30}$$

For the four-terminal network N_{22}, the solution method is same to four-terminal network N_{11}. The calculation process l_1 and Z_{HBX} are changed to l_2 and Z_{KBX} simply. For the four- terminal network N_{11}, $\dot{U}_{1C}$ is calculated as the terminal-voltage. And for the four- terminal network N_{22}, $\dot{U}_{1C}$ is calculated as the voltage at the beginning. That is to say, the energy transfer direction of the two four-terminal network has changed. And for a four-terminal network when the energy transfer direction is changed, the position of the four-terminal network coefficient matrix and will also exchange. So the coefficients of four-terminal network N_{22} can be expressed as,

$$\begin{cases} D_{22} = 2\cosh \gamma l_2 \\ B_{22} = Z_{\mathrm{B1}} \cosh \gamma l_2 + Z_{\mathrm{B2}} \sinh \gamma l_2 \\ C_{22} = \dfrac{1}{Z_{\mathrm{B2}}} \sinh \gamma l_2 \\ A_{22} = \dfrac{1}{2}\left(\dfrac{Z_{\mathrm{B1}}}{Z_{\mathrm{B2}}} \sinh \gamma l_2 + \cosh \gamma l_2 \right) \end{cases} \tag{31}$$

Substituting (18) in (30) and (31), then the results are substituted into the formula (10). The four-terminal network coefficient of symmetrical rail that track circuit in broken state is obtained as follows,

$$\begin{cases} A = \cosh \gamma l + 2E\sqrt{1+P}\cosh(\gamma l_1)\sinh \gamma l_2 \\ B = Z_{\mathrm{B}}[\sinh \gamma l + 2E\sqrt{1+P}\cosh(\gamma l_1)\cosh \gamma l_2] \\ C = \dfrac{1}{Z_{\mathrm{B}}}[\sinh \gamma l + 2E\sqrt{1+P}\sinh(\gamma l_1)\sinh \gamma l_2] \\ D = \cosh \gamma l + 2E\sqrt{1+P}\sinh(\gamma l_1)\cosh \gamma l_2 \end{cases} \tag{32}$$

3 Broken Mode Choke Transformer Combined with Track Circuit to Solve a Four-terminal Network Coefficients

The equivalent circuit of the combination of track circuit in broken state and choke transformer is shown in Fig.6. The rail lines were connected with the sender and receiver choke transformer respectively at the start and the end terminal [20].

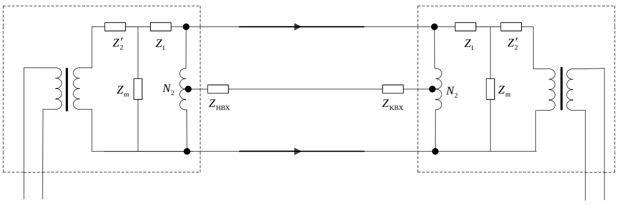

Fig. 6 Equivalent circuit of the choke transformer combined with track circuit in broken state

The transmission terminal choke transformer is represented by four-terminal network N_{FE}, the receiving terminal of the choke transformer is represented by four-terminal network N_{JE}, the middle part of the rail network circuit is represented by a four-terminal network N_G. And then Fig. 6 can be equivalent to Fig. 7.

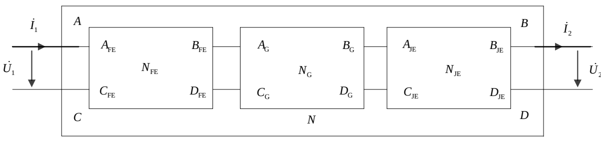

Fig. 7. Cascade four-terminal network of the choke transformer and the track circuit in broken state

It can be obtained from Fig. 7 that overall coefficient of a four-terminal network is:

$$\begin{bmatrix} A & B \\ C & D \end{bmatrix} = \begin{bmatrix} A_{\mathrm{FE}} & B_{\mathrm{FE}} \\ C_{\mathrm{FE}} & D_{\mathrm{FE}} \end{bmatrix} \cdot \begin{bmatrix} A_{\mathrm{G}} & B_{\mathrm{G}} \\ C_{\mathrm{G}} & D_{\mathrm{G}} \end{bmatrix} \begin{bmatrix} A_{\mathrm{JE}} & B_{\mathrm{JE}} \\ C_{\mathrm{JE}} & D_{\mathrm{JE}} \end{bmatrix} \tag{33}$$

Substituting (1) and (32) in (33), the overall four-terminal network coefficient of the track circuit in broken state can be expressed as,

$$\begin{cases} A = \left(\dfrac{0.034}{Z_{\mathrm{B}}} + 0.425Z_{\mathrm{B}} \right)\sinh(\gamma l) + 0.850Z_{\mathrm{B}}E\sqrt{1+P}\cosh(\gamma l_1) \bullet \\ \quad \cosh(\gamma l_2) + \dfrac{0.068}{Z_{\mathrm{B}}}E\sqrt{1+P}\sinh(\gamma l_1)\sinh(\gamma l_2) + \\ \quad 2.028E\sqrt{1+P}\cosh(\gamma l_1)\sinh(\gamma l_2) + 0.028E\sqrt{1+P} \bullet \\ \quad \sinh(\gamma l_1)\cosh(\gamma l_2) + 1.028\cosh(\gamma l) \\ B = \left(\dfrac{0.001}{Z_{\mathrm{B}}} + 1.014Z_{\mathrm{B}} \right)\sinh(\gamma l) + 2.028Z_{\mathrm{B}}E\sqrt{1+P}\cosh(\gamma l_1) \bullet \\ \quad \cosh(\gamma l_2) + \dfrac{0.002}{Z_{\mathrm{B}}}E\sqrt{1+P}\sinh(\gamma l_1)\sinh(\gamma l_2) + \\ \quad 0.068E\sqrt{1+P}\cosh(\gamma l_1)\sinh(\gamma l_2) + 0.068E\sqrt{1+P} \bullet \\ \quad \sinh(\gamma l_1)\cosh(\gamma l_2) + 0.068\cosh(\gamma l) \\ C = \left(\dfrac{1.014}{Z_{\mathrm{B}}} + 0.178Z_{\mathrm{B}} \right)\sinh(\gamma l) + 0.356Z_{\mathrm{B}}E\sqrt{1+P}\cosh(\gamma l_1) \bullet \\ \quad \cosh(\gamma l_2) + \dfrac{2.028}{Z_{\mathrm{B}}}E\sqrt{1+P}\sinh(\gamma l_1)\sinh(\gamma l_2) + \\ \quad 0.850E\sqrt{1+P}\cosh(\gamma l_1)\sinh(\gamma l_2) + 0.850E\sqrt{1+P} \bullet \\ \quad \sinh(\gamma l_1)\cosh(\gamma l_2) + 0.850\cosh(\gamma l) \\ D = \left(\dfrac{0.034}{Z_{\mathrm{B}}} + 0.425Z_{\mathrm{B}} \right)\sinh(\gamma l) + 0.850Z_{\mathrm{B}}E\sqrt{1+P} \bullet \\ \quad \cosh(\gamma l_1)\cosh(\gamma l_2) + \dfrac{0.068}{Z_{\mathrm{B}}}E\sqrt{1+P}\sinh(\gamma l_1)\sinh(\gamma l_2) + \\ \quad 0.028E\sqrt{1+P}\cosh(\gamma l_1)\sinh(\gamma l_2) + 2.028E\sqrt{1+P} \bullet \\ \quad \sinh(\gamma l_1)\cosh(\gamma l_2) + 1.028\cosh(\gamma l) \end{cases}$$

4 Simulation Analysis on Transmission Characteristics of Track Circuit in Broken State

MATLAB is the abbreviation of Matrix Laboratory, and it was developed in around 1980. After continuous development, the MATLAB has more than just a "matrix laboratory", and has become a widely used in engineering calculations and numerical analysis in the field of the new advanced language [21].

The process is simulated with a MATLAB language program. Already know rail impedance $z = 0.62\angle 42°$ */km*, the track relay must be ensured to fall off when the track circuit in broken state. The voltage signal receiving coil terminals of the choke transformer is $\dot{U}_2 = 0.57498\angle 73.23°$ V, and the current is $\dot{I}_2 = 0.06821\angle 65.07°$ A. The change curve of signal coil of the sending terminal choke transformer's voltage and current with broken rail position, surface conductance and ballast resistance are emulated. Simulation results are shown in Fig. 8 to 13.

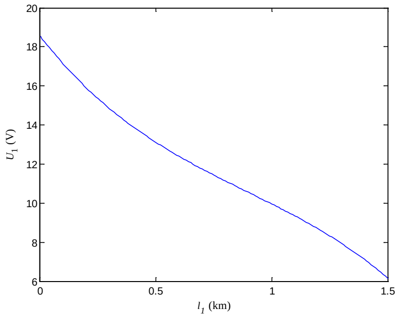

Fig. 8 The variation curve of the sending terminal voltage with the position of the broken rail

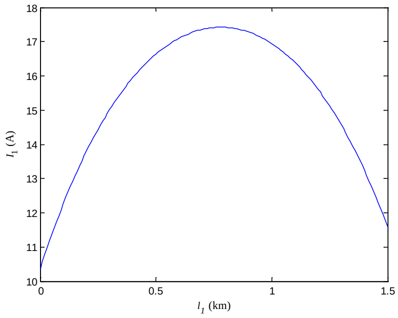

Fig. 9 The variation curve of the sending terminal current with the position of the broken rail

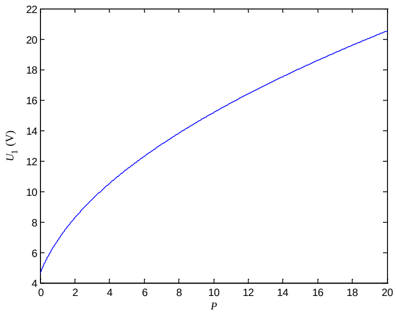

Fig. 10 The variation curve of the sending terminal voltage with the conductivity coefficient

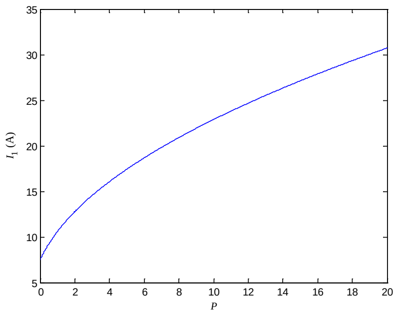

Fig. 11 The variation curve of the sending terminal current with the conductivity coefficient

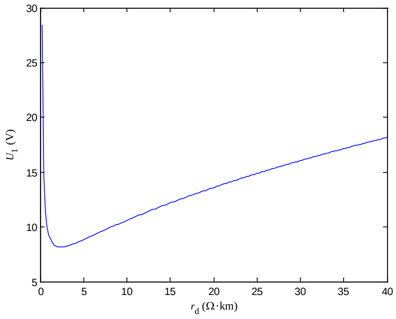

Fig. 12 The variation curve of the sending terminal voltage with the ballast resistance

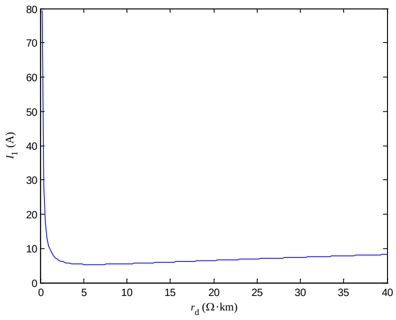

Fig. 13 The variation curve of the sending terminal current with the ballast resistance

Fig. 8 and 9 shows in ballast resistance r_d=0.6$\Omega \cdot km$ and rail surface conductance coefficient P=5, the broken rail position l_1 as a variable, and then simulate the transmission characteristics of the track circuit. Fig. 10 and 11 shows in ballast resistance r_d=0.6$\Omega \cdot km$ and the broken rail position l_1=0.75km, P is used as the variable of the rail surface conductance coefficient, and then simulate the transmission characteristics of the track circuit. Fig. 12 and 13 shows in broken rail position l_1=0.75km and rail surface conductance coefficient P=5, the ballast resistor r_d as a variable, and then simulate the transmission characteristics of the track circuit.

Based on the above simulation results, the broken rail sensitivity K_{OP} can be analyzed.

$$K_{\mathrm{OP}} = \frac{|Z_{\mathrm{DUAN}}|}{N|Z_{\mathrm{TIAO}}|} \tag{34}$$

Where, Z_{TIAO} is the transfer impedance of track circuit under the condition of the most unfavorable adjustment state, Z_{DUAN} is the transfer impedance of track circuit in broken state under the condition of the most disadvantage, and N is the number of devices in the track circuit.

Because the ratio of the terminal voltage to the receiving terminal current is represented as Z_{TIAO} or Z_{DUAN}. It is shown that the receiving terminal current is also increased with the increase of the surface conductance coefficient from the Fig. 10 and 11. So Z_{DUAN} increases with the increase of the surface conductivity coefficient, and the K_{OP} increases correspondingly. So the measures to improve the sensitivity of the broken rail are: appropriate to reduce the length of the track circuit, increase the ballast resistance and increase the surface conductivity coefficient.

5 Conclusion

First of all, the system structure of 25Hz phase-sensitive track circuit is introduced, and its working principle is described in this paper. Then the choke transformer and the track circuit is modeled, and the equivalent circuit for four terminal network's coefficient is solved, the overall choke transformer and track circuit composed of four-terminal network's coefficients is solved. Finally, MATLAB is used to program the simulation. The simulation results can be seen that the transmission characteristics and the broken rail position l_1, the surface of the rail conductance coefficient P and the ballast resistance r_d of track circuit is related closely. Through the analysis of the simulation results, and finally come to improve the sensitivity of the relevant measures. Because the track is longer, the ballast resistance is smaller, transfer resistance Z_{TIAO} in adjustment state is greater and the broken rail sensitivity K_{OP} is smaller. It is possible to reduce the length of the track properly and increase the ballast resistance to improve the sensitivity of broken rail. And because the receiving terminal current is decreased with the increase of the surface conductivity. Therefore, the transfer impedance Z_{DUAN} increases with the increase of the surface conductivity and broken rail sensitivity K_{OP} is also increased accordingly. So increasing the conductivity of the track surface is also an effective measure to improve the sensitivity of the broken rail. Improve the sensitivity of broken rail can ensure train operation safety effectively. And put forward the improvement method of keeping the stability of the rail and energy saving.

References:

[1] S.H. Zhu, Comparison of UM-71 and ZPW-2000A track circuit, *Railway Signalling & Communication*, Vol.44, No.7, 2008, pp. 17-18.

[2] J. X. Xu et. al., ZPW2000A Joint-less Track Circuit System Modeling and Simulation Considering Adjacent Signal Interference, *in Proceeding of the 32nd Chinese Control Conference*, 2013, pp. 8780-8787.

[3] S. Shooman, Broken Rail Detection Without Track Circuits, *in Proceeding of the Joint University of Illinois/AAR/FRA Workshop on Rail Defect Detection and Removal Policies and Broken Rail Detection Technologies*, 1997.

[4] G. Zumpano et. al., A new damage detection technique based on wave propagation for rails, *International Journal of Solids and Structures,* Vol. 43, No. 5, 2006, pp. 1023-1046.

[5] T. Devin et. al., Diffuse ultrasonic backscatter measurements for monitoring stress in rail, *The Journal of the Acoustical Society of America,* Vol. 132, No. 3, 2012, pp. 1961-1961.

[6] L. Oukhellou et. al., Dedicated sensor and classifier of rail head defects, *Control Engineering Practice,* Vol. 7, No. 1, 1999, pp. 57-61.

[7] A. D. Kersey et. al., High-resolution fibre-grating based strain sensor with interferometric wavelength-shift detection, *Electronics Letters, Vol. 28,* No. 3, 1992, pp. 236-238.

[8] X. Dai et. al., The Condition Monitoring Based on Fiber Bragg Grating of Continuously Welded Line Track at Subway Viaduct Section of a Certain City, *in Proceeding of the Fifth International Conference on Intelligent Systems Design and Engineering Applications*, 2014, pp. 1010-1013.

[9] L. H. Peter, Alternating-current track circuiting, *Journal of the Institution of Electrical Engineers*, Vol. 58, No. 292, 1920, pp. 491-506.

[10] P. Y. Liu, On the Simulation of the Characteristics of Electric Track Circuit, *Urban Mass Transit*, Vol. 15, No. 12, 2011, pp. 23-28.

[11] N. Nikolov, Study on Centre-fed Boundless Track Circuits, *IEE Proceedings-Electric Power Applications*, Vol. 152, No. 5, 2005, pp. 1049-1054.

[12] M. X. Tian, Analysis on the broken rail mode of a track circuit of center-fed double-side current-received type, *China railway science*, Vol. 31, No. 6, 2010, pp. 103-108.

[13] A. Mariscotti, Modeling of audio frequency track circuits for validation, tuning, and conducted interference prediction, *IEEE Transactions on Intelligent Transportation Systems*, Vol. 11, No. 1, 2010, pp. 52-60.

[14] A. Hernandez, FPGA-Based Track Circuit for Railways Using Transmission Encoding, *IEEE Transactions on Intelligent Transportation Systems*, Vol. 13, No. 2, 2012, pp. 437-448.

[15] G. Z. Mao, The modeling and simulation of track circuit, *Electric Drive for Locomotives*, Vol. 12, No. 1, 2004, pp. 41-46.

[16] M. G. Cao, Research of modeling and test on impedance bond in the high speed railway, *PhD. Thesis*, Beijing Jiaotong University, 2014.

[17] Z. G. Wang et. al., Test and adjustment of 25Hz phase sensitive track circuit, *Railway signalling & communication*, Vol. 40, No. 3, 2004, pp. 28-30.

[18] H. John et. al., Rail track distributed transmission line impedance and admittance: theoretical modeling and experimental results, *IEEE Transactions on Vehicular Technology*, Vol. 42, No. 2, 1993, pp. 225-241.

[19] X. l. Du, Calculation of the Impedance of a Rail Track with Earth Return for the High-Speed Railway Signal Circuit Using Finite-Element Method, *IEEE Transactions on Magnetics*, Vol. 51, No. 3, 2015, pp. 1-4.

[20] X. J. Yuan, Testing and adjustment of 97 type 25Hz phase sensitive track circuit (three), *Railway signalling & communication*, Vol. 43, No. 2, 2007, pp. 23-25.

[21] B. Moler et. al., Numerical computing with MATLAB, *Beihang university press*, Chap.2, 2013.